University of Zurich, the Peabody Museum, Harvard University, and the Royal Africa Museum, Tervuren. Midsagittal landmarks used were nasion, glabella, bregma, lambda, inion, opisthion, basion, sphenobasion, staphylion, prosthion and nasospinale; paired landmarks (left and right sides taken when possible) were maxillofrontale, supraorbitale, orbitale, frontomalare orbitale, zygomaxillare, jugale, foramen infraorbitale, M^2 most buccal point, foramen stylomastoideum, foramen caroticum, foramen ovale, asterion, porion and pterion.

Received 17 September 2004; accepted 25 January 2005; doi:10.1038/nature03397.

1. Brunet, M. *et al.* A new hominid from the Upper Miocene of Chad, Central Africa. *Nature* **418,** 145–151 (2002).
2. Brunet, M. *et al.* New material of the earliest hominid from the Upper Miocene of Chad. *Nature* doi:10.1038/nature03392 (this issue).
3. Vignaud, P. *et al.* Geology and palaeontology of the Upper Miocene Toros-Menalla hominid locality, Chad. *Nature* **418,** 152–155 (2002).
4. Wolpoff, M. H., Senut, B., Pickford, M. & Hawks, J. *Sahelanthropus* or '*Sahelpithecus*'? *Nature* **419,** 581–582 (2002).
5. Brunet, M. *et al. Sahelanthropus* or '*Sahelpithecus*'? (Reply). *Nature* **419,** 582 (2002).
6. White, T. Early hominids—diversity or distortion? *Science* **299,** 1994–1997 (2003).
7. McCarthy, R. C. & Lieberman, D. E. Posterior maxillary (PM) plane and anterior cranial architecture in primates. *Anat. Rec.* **264,** 247–260 (2001).
8. Enlow, D. H. *Facial Growth* (Saunders, Philadelphia, 1990).
9. Rohlf, F. J. & Slice, D. Extensions of the Procrustes method for the optimal superimposition of landmarks. *Syst. Zool.* **39,** 40–59 (1990).
10. Zollikofer, C. P. E. & Ponce de León, M. S. Visualizing patterns of craniofacial shape variation in *Homo sapiens*. *Proc. R. Soc. Lond. B* **269,** 801–807 (2002).
11. Penin, X., Berge, C. & Baylac, M. Ontogenetic study of the skull in modern humans and the common chimpanzees: neotenic hypothesis reconsidered with a tridimensional Procrustes analysis. *Am. J. Phys. Anthropol.* **118,** 50–62 (2002).
12. Aiello, L. & Dean, C. *An Introduction to Human Evolutionary Anatomy* (Academic, London, 1990).
13. Kimbel, W. H., Johanson, D. & Rak, Y. *The Skull of Australopithecus afarensis* (Oxford Univ. Press, New York, 2004).
14. Wood, B. & Richmond, B. G. Human evolution: taxonomy and paleobiology. *J. Anat.* **196,** 19–60 (2000).
15. Haile-Selassie, Y. Late Miocene hominids from the Middle Awash, Ethiopia. *Nature* **412,** 178–181 (2001).
16. Pickford, M., Senut, B., Gommery, D. & Treil, J. Bipedalism in *Orrorin tugenensis* revealed by its femora. *C. R. Palevol.* **1,** 191–203 (2002).
17. Strait, D. S. & Ross, C. F. Kinematic data on primate head and neck posture: implications for the evolution of basicranial flexion and an evaluation of registration planes used in paleoanthropology. *Am. J. Phys. Anthropol.* **108,** 205–222 (1999).
18. Graf, W., de Waele, C. & Vidal, P. P. Functional anatomy of the head–neck movement system of quadrupedal and bipedal mammals. *J. Anat.* **186,** 55–74 (1995).
19. Lieberman, D. E., Ross, C. F. & Ravosa, M. J. The primate cranial base: ontogeny, function, and integration. *Yb. Phys. Anthropol.* **43,** 117–169 (2000).
20. Holloway, R. L., Broadfield, D. C., Yuan, M. S., Schwartz, J. H. & Tattersall, I. *The Human Fossil Record Vol. 4: Brain Endocasts* (Wiley, New York, 2004).
21. Kimbel, W. H., White, T. D. & Johanson, D. C. Cranial morphology of *Australopithecus afarensis*: a comparative study based on a composite reconstruction of the adult skull. *Am. J. Phys. Anthropol.* **64,** 337–388 (1984).
22. Gonzalez, R. C. & Woods, R. E. *Digital Image Processing* (Prentice Hall, Upper Saddle River, New Jersey, 2002).
23. Zollikofer, C. P. E., Ponce de León, M. S. & Martin, R. D. Computer-assisted paleoanthropology. *Evol. Anthropol.* **6,** 41–54 (1998).
24. Ponce de León, M. S. & Zollikofer, C. P. E. New evidence from Le Moustier. 1: Computer-assisted reconstruction and morphometry of the skull. *Anat. Rec.* **254,** 474–489 (1999).
25. Delattre, A. & Fenart, R. *L'hominisation du Crâne Étudiée par la Méthode Vestibulaire* (CNRS, Paris, 1960).
26. Zollikofer, C. P. E., Ponce de León, M. S., Martin, R. D. & Stucki, P. Neanderthal computer skulls. *Nature* **375,** 283–285 (1995).

Supplementary Information accompanies the paper on **www.nature.com/nature**.

Acknowledgements We thank the Chadian Authorities (Ministère de l'Éducation Nationale de l'Enseignement Supérieur et de la Recherche, Université de N'Djaména, Centre National d'Appui à la Recherche au Tchad), the Ministère Français de l'Éducation Nationale (Faculté des Sciences, Université de Poitiers), Ministère de la Recherche (CNRS: Département SDV & ECLIPSE), Ministère des Affaires Étrangères (DCSUR Commission des fouilles, Paris, et SCAC Ambassade de France à N'Djaména), the Revealing Hominid Origins Initiative (co-principal investigators F. C. Howell and T. D. White), the American School of Prehistoric Research, Harvard University, and the Swiss National Science Foundation, for support; the MultiMedia Laboratorium, University of Zürich (P. Stucki); EMPA Dübendorf, Switzerland, for industrial computed tomography (A. Flisch); all the MPFT members; and S. Riffaut, X. Valentin, G. Florent and C. Noël for technical support and administrative guidance.

Competing interests statement The authors declare that they have no competing financial interests.

Correspondence and requests for materials should be addressed to M.B. (michel.brunet@univ-poitiers.fr).

Evolutionary diversification of TTX-resistant sodium channels in a predator–prey interaction

Shana L. Geffeney[1], Esther Fujimoto[1]*, Edmund D. Brodie III[2], Edmund D. Brodie Jr[1] & Peter C. Ruben[1]

[1]*Department of Biology, Utah State University, Logan, Utah 84322-5305, USA*
[2]*Department of Biology, Indiana University, Bloomington, Indiana 47405-3700, USA*

* Present address: Department of Neurobiology and Anatomy, University of Utah School of Medicine, Salt Lake City, Utah 84123-3401, USA

Understanding the molecular genetic basis of adaptations provides incomparable insight into the genetic mechanisms by which evolutionary diversification takes place. Whether the evolution of common traits in different lineages proceeds by similar or unique mutations, and the degree to which phenotypic evolution is controlled by changes in gene regulation as opposed to gene function, are fundamental questions in evolutionary biology that require such an understanding of genetic mechanisms[1–3]. Here we identify novel changes in the molecular structure of a sodium channel expressed in snake skeletal muscle, $tsNa_V1.4$, that are responsible for differences in tetrodotoxin (TTX) resistance among garter snake populations coevolving with toxic newts[4]. By the functional expression of $tsNa_V1.4$, we show how differences in the amino-acid sequence of the channel affect TTX binding and impart different levels of resistance in four snake populations. These results indicate that the evolution of a physiological trait has occurred through a series of unique functional changes in a gene that is otherwise highly conserved among vertebrates.

Identifying the connection between genotype and phenotype is the critical step uniting evolutionary studies of phenotypic diversity with more proximate investigations of development, function and structure[5–8]. One emerging picture is that the process of adaptive radiation might be more predictable at the genetic level than previously imagined and that the regulation of genes of major effect rather than the alteration of functional products might explain much phenotypic diversity[1,3]. Identifying the genetic basis of bill differences in Galapagos finches[6] and eyespot patterns in butterflies[5], and the loss of pelvic spines in sticklebacks[7] or eyes in cave-dwelling fish[8], has led to an increased understanding about how evolution generates convergent and divergent traits at the molecular level. In each of these cases, ecologically important morphological differences between lineages are explainable through changes in the regulation of single genes in developing tissues. However, functional changes in the protein-coding regions of structural genes explain adaptive differences in other cases, including cryptic pigmentation in rodents[9] and pesticide resistance in insects[10].

Coevolution between the garter snake *Thamnophis sirtalis* and its toxic prey, the newt *Taricha granulosa*, has resulted in geographic variability in a physiological trait, resistance to TTX in predator lineages[4]. Tetrodotoxin causes paralysis and death by binding to the outer pore of voltage-gated sodium channels and blocking nerve and muscle fibre activity[11]. Some populations of *Taricha* have extremely high levels of TTX in their skin that provide an almost impenetrable defence against predators[12], yet elevated TTX resistance has evolved at least twice within the radiation of *T. sirtalis*[4,13]. This physiological adaptation is at least partly accounted for by the expression of TTX-resistant sodium channels in the skeletal muscle of resistant garter snakes[14]. Here we identify the molecular mechanisms underlying this diversification.

The extent to which TTX affects nerve and muscle tissue is

determined by the sodium channel isoforms expressed in the tissue. TTX-sensitive members of the gene family that encodes voltage-gated sodium channels are distinguished by the presence of an aromatic amino acid in the outer pore of domain I that is responsible for high-affinity TTX binding[15]. In tetrodotoxic animals, TTX resistance has been linked to the substitution of non-aromatic amino acids at this critical position in domain I in TTX-sensitive members of the sodium channel gene family[16,17], although mutational analysis has shown that substitutions at other positions in the outer pore also can alter TTX binding[18,19]. In rats, the TTX sensitivity of skeletal muscle tissue is altered during development and after denervation as a result of changes in the expression levels of TTX-resistant ($rNa_V1.5$) and TTX-sensitive ($rNa_V1.4$) members of the sodium channel gene family[20,21]. TTX resistance in garter snakes might be due to a change in sodium channel gene expression[22] or mutations in TTX-sensitive members of the sodium channel gene family[23].

We identified the TTX-resistant sodium channel gene expressed in skeletal muscle tissue by making a complementary DNA library from skeletal muscle of a snake from a population with elevated TTX resistance ('Benton'). We screened the library with probes designed to identify clones with skeletal and cardiac muscle sodium channel sequences ($Na_V1.4$ and $Na_V1.5$) and sequenced the positive cDNA library clones revealing one open-reading frame of 5,625 nucleotides that encodes an 1,875-amino-acid protein. Phylogenetic analysis of the protein-coding region of the nucleotide sequence revealed a well-supported association of our sequence with other $Na_V1.4$ genes (see Supplementary Fig. S1 and Supplementary Methods) and we refer to this channel as $tsNa_V1.4$. The predicted protein sequence of $tsNa_V1.4$ has a tyrosine residue in the domain I position that is responsible for high-affinity TTX binding[15]. However, two novel amino-acid substitutions were found in other regions important for TTX binding and pore structure, the pore helix and β-strand of the domain IV outer pore[19,24] (Fig. 1).

Sequences of $tsNa_V1.4$ from three other snake populations (Fig. 1a) with different levels of resistance to TTX all have tyrosine in the domain I position responsible for high-affinity TTX binding. There are no sequence differences between the four populations in regions encoding the pore helix, selectivity filter and β-strand of domains I, II and III. The predicted amino-acid sequence of the pore helix, selectivity filter and β-strand of domain IV from a non-resistant population (Bear Lake) matches that of human and rat $Na_V1.4$, indicating that it might be a TTX-sensitive channel. However, sequences from the resistant snake populations have unique amino-acid substitutions in the domain IV outer pore (Fig. 1). Because we sequenced cDNA from mRNA transcripts, we cannot eliminate the possibility that these differences reflect post-transcriptional modifications. However, alternative splicing has never been detected for $Na_V1.4$ (refs 25, 26) and is unlikely to explain the pattern of substitutions observed in different populations.

To test whether observed differences in the amino-acid sequence alter the TTX-sensitivity of $tsNa_V1.4$, we expressed the channels in *Xenopus* oocytes. We tested both $tsNa_V1.4$ and human–snake chimaeras in which the human $Na_V1.4$ sequence had the regions that form the outer pore, the S5–S6 linkers from domains I–IV, replaced with $tsNa_V1.4$ sequence (see Supplementary Fig. S2). We began with constructs with the $tsNa_V1.4$ sequence from Benton, then mutated individual amino acids to match pore substitutions in other snake populations, and measured the effects of these changes in the domain IV pore sequence on TTX sensitivity.

Channels with snake sequences were not more resistant to TTX block than chimaeric channels, indicating that regions outside the S5–S6 linkers might not increase the TTX resistance of snake channels (Fig. 2a, Table 1). Chimaeric channels with different domain IV pore sequences had markedly different TTX-binding affinities (Fig. 2b, d, Table 1). The TTX concentration at which 50% of sodium channels are blocked by TTX (K_d) for a chimaeric channel with the Bear Lake sequence was comparable to K_d values for TTX-sensitive $Na_V1.4$ from rat (5 nM TTX) and human (25 nM TTX)[27]. The K_d for the Willow Creek chimaera was three orders of magnitude greater than the K_d for Bear Lake and greater than the K_d values for TTX-resistant, mammalian cardiac channels, $Na_V1.5$ (rat, 2.0 μM TTX; human, 6.0 μM TTX)[27]. The binding affinities for the

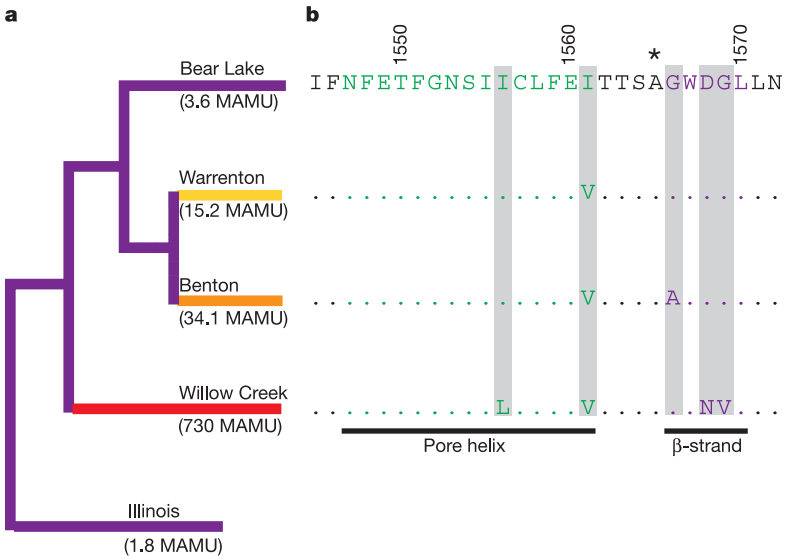

Figure 1 Amino-acid sequence differences for four snake populations. **a**, Phylogeographic relationships based on mitochondrial DNA analysis of 19 North American populations of *Thamnophis sirtalis* indicate separate origins of elevated resistance to TTX in the Willow Creek population compared with populations from Benton and Warrenton[4,13]. Bear Lake is from a third lineage and is not resistant to TTX. Whole-animal TTX resistance for each population is reported in mass-adjusted mouse units (MAMU); branch colours reflect statistically distinguishable levels of resistance[4]. Whole-animal TTX resistance was measured as a mass-adjusted dose of TTX (MAMU) that produced an average of 50% decrease in snake sprint speed in each population. **b**, Amino-acid alignment of part of the domain IV S5–S6 linker that affects TTX binding from $tsNa_V1.4$. Green, pore α-helix; purple, β-strand; asterisk, selectivity filter. Dots indicate identical amino acids and grey shading highlights sequence differences between populations. Despite independent evolutionary histories, all resistant snakes share the substitution of valine for isoleucine at position 1,561.

Warrenton and Benton chimaeras were intermediate to those of the other populations (Fig. 2b, Table 1). The TTX binding affinities of cloned channels with the amino-acid sequences found in the four populations are closely correlated with skeletal-muscle-fibre and whole-animal resistance of snakes from the same populations (compare Fig. 1a with Fig. 3)[14]. This correlation indicates that functional changes in $tsNa_V1.4$ are largely responsible for the differences in TTX resistance observed in snake populations.

The functional consequences of the amino-acid substitutions can be understood within the context of recent models of pore structure. A hydroxyl group on TTX interacts with an aspartic acid residue in the domain IV outer pore of rat $Na_V1.4$ (ref. 28). When this charged amino acid is neutralized by substituting asparagine at this position, the TTX binding affinity of the channel is decreased by two orders of magnitude[28,29]. Charge neutralization of the equivalent residue (position 1,568) in the Willow Creek sequence, in which aspartic acid is changed to asparagine, might similarly affect the electrostatic interaction between TTX and this pore residue[28]. The amino-acid changes in Warrenton and Benton might affect TTX binding by altering pore structure. The substitutions are in a region of the S5–S6 linker where the protein forms a sharp bend and interactions between hydrophobic residues from the pore helix and the β-strand stabilize the structure of the mouth of the pore[24]. Even a single change from isoleucine to valine at position 1,561 in the domain IV pore helix doubles the K_d of the Warrenton chimaera compared with that of the Bear Lake chimaera (Fig. 2b, Table 1). When this valine at position 1,561 is restored to isoleucine in the Willow Creek chimaera, the K_d value of the channel is halved (Fig. 2c, Table 1).

Table 1 **K_d values and 95% confidence limits for all channels**

Channel type	K_d ± 95% confidence limits (nM)
Bear Lake $tsNa_V1.4$	20 ± 5.8
Bear Lake chimaera	22 ± 6.6
Benton $tsNa_V1.4$	120 ± 41
Benton chimaera	210 ± 60
Warrenton chimaera	44 ± 4.2
Willow Creek chimaera	$12{,}000^{+2{,}000}_{-2{,}900}$
Willow Creek chimaera V1561I	5,900 ± 1,400

The TTX concentration that blocked 50% of the channels (K_d) for each channel type was calculated from pooled channel data (see Methods).

Our results suggest that elevated TTX resistance has repeatedly evolved in snake populations through a variety of mutations in the gene that encodes $tsNa_V1.4$ and that these mutations alter the TTX-binding affinity of the channel by several orders of magnitude. Some of the changes observed here are unique to specific lineages (for example, glycine to alanine at position 1,566 in the Benton population, and three of the four substitutions observed in the Willow Creek population) and confer very large differences in TTX binding affinity. One mutation, which alters isoleucine to valine at position 1,561, might represent parallel evolution at that site in resistant populations, although the functional effect of the substi-

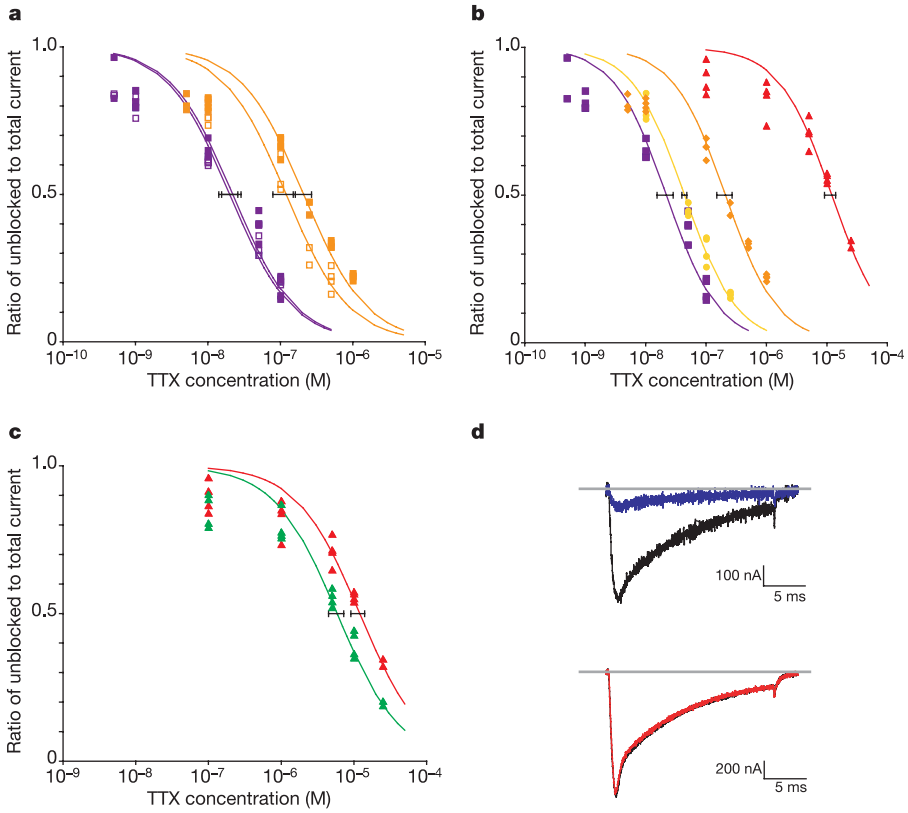

Figure 2 The effect of different TTX concentrations on $tsNa_V1.4$ and snake–human chimaeric channels. **a**–**c**, Each symbol corresponds to the ratio of unblocked to total current for an oocyte expressing the indicated channel and exposed to one TTX concentration. The TTX concentration that blocked 50% of the channels (K_d) for each channel type was calculated from pooled channel data (see Methods). K_d values (±95% confidence limits) are shown for each channel type with a black bar. The lines represent the equation fitted to the data with the estimated K_d for each channel type. **a**, Channels with entirely snake sequence (open squares) are not more resistant to TTX block than chimaeric channels (filled squares). Purple, Bear Lake; orange, Benton. **b**, Chimaeric channels with the domain IV S5-S6 linker sequence of each of the four populations are blocked by different TTX concentrations. Purple, Bear Lake; yellow, Warrenton; orange, Benton; red, Willow Creek. **c**, Changing a valine (red points and line) to an isoleucine (green points and line) at position 1,561 in the domain IV S5–S6 linker of the Willow Creek chimaera halves the K_d value of the channel. **d**, Current recordings from chimaeric channels expressed in *Xenopus* oocytes before (black lines) and after (red and blue lines) the addition of 100 nM TTX to the external solution. Channels with the domain IV S5–S6 linker sequences of Bear Lake (top panel, blue) are blocked by 100 nM TTX and Willow Creek chimaeric channels (bottom panel, red) are not. Grey bar, zero current.

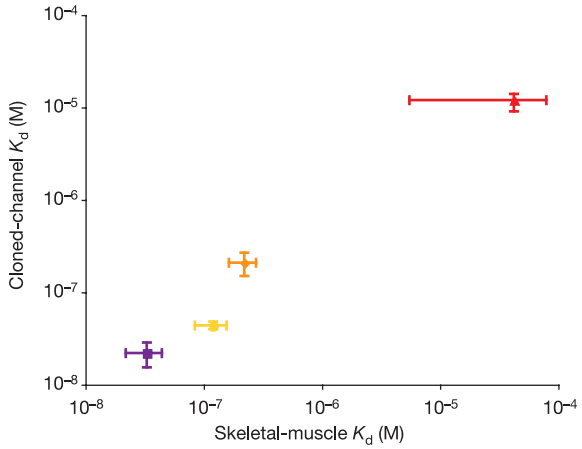

Figure 3 TTX binding affinity of cloned channels compared with skeletal muscle in four snake populations. TTX binding affinity is measured as K_d, the TTX concentration required to block 50% of channels. K_d values (±95% confidence limits) for skeletal muscle were estimated from action potential rise rates recorded in skeletal muscle fibres of snakes from the four populations[14]. K_d values (±95% confidence limits) for cloned channels were estimated from currents recorded from human–snake chimaeric channels expressed in *Xenopus* oocytes with the Bear Lake (purple), Warrenton (yellow), Benton (orange) and Willow Creek (red) sequences in the domain IV S5–S6 linker. Linear regression indicates a significant relationship between the K_d values measured from the cloned channels and skeletal muscle fibres ($F(1,3) = 17{,}197.116$, $R^2=1$, $P < 0.0001$).

tution is too small (only a twofold change in binding affinity) to explain much of the phenotypic differences observed. Our current data do not allow us to determine unequivocally whether the valine is derived or ancestral at this site (Fig. 1), although the isoleucine at this position is conserved in all other known vertebrate $Na_V1.4$ sequences. Additionally, the ancestral phenotypic state for *T. sirtalis*, and the genus *Thamnophis* in general, is high sensitivity to TTX, indicating that it is unlikely they could all have valine at this position, which produces a decrease in the binding affinity of the channel for TTX.

Our conclusions are based on analyses of differences in cDNA sequence that cannot be unequivocally attributed to changes in genomic DNA. A complete analysis of the relative importance of parallel genotypic evolution in this system will require much broader sampling of genomic DNA across a range of lineages, but the functional analyses of expressed proteins reported here indicate that both unique and parallel molecular changes might have a function in the diversification of TTX resistance in garter snakes. Although the changes in $tsNa_V1.4$ seem to explain much of the variation in TTX resistance among garter snake populations, considerable variation within populations has been observed that cannot be explained by the genetic mechanism reported here. These individual differences might be explained by alterations in the protein-coding regions of other genes or by differences in gene regulation, including that of $tsNa_V1.4$. Nonetheless, our study shows that adaptive diversification of a quantitative trait within a species proceeds through the variable effects of substitution of different amino acids at a highly conserved locus. □

Methods

cDNA library construction and screening

Total RNA was extracted from a skeletal muscle tissue sample from a 'Benton' snake (Benton County, Oregon; deposited in the University of Texas at Arlington Collection of Vertebrates, UTA R 52941) using TRIzol reagent as recommended by the manufacturer (Invitrogen). To construct the cDNA library, poly(A)$^+$ RNA was isolated by Oligotex purification (Qiagen), then primed with random and oligo(dT) primers, and the cDNA was cloned into *Eco*RI-digested Lambda ZAP (Stratagene). The library was screened with random-primed, radiolabelled probes (Prime-It; Stratagene). One set of probes was developed from reverse transcriptase-mediated polymerase chain reaction (RT–PCR) products amplified from snake skeletal muscle tissue first-strand cDNA (SuperScript, Invitrogen) with the use of primer pairs designed from conserved $Na_V1.4$ and $Na_V1.5$ sequences (Supplementary Methods). All positive clones were sequenced with an ABI 373 or ABI 377 automated sequencer (Applied Biosystems) and aligned with Sequencher 3.1 software (Gene Codes Corp.). A $Na_V1.5$-specific probe was prepared from RT–PCR products amplified from snake heart tissue first-strand cDNA (SuperScript) with the use of one primer pair (Supplementary Methods). No positive clones were identified with this probe.

RT–PCR

All other snake sequences were obtained from a skeletal muscle tissue sample of one individual from each population, 'Bear Lake' (Bear Lake County, Idaho), 'Warrenton' (Clatsop County, Oregon) and 'Willow Creek' (Sonoma County, California). Total RNA was extracted and cDNA was synthesized as above. PCR primers listed in Supplementary Methods were used to amplify the open-reading frame. RT–PCR products were cloned into pCR-Blunt (Invitrogen), sequenced and aligned.

Expression constructs

The full-length $tsNa_V1.4$ construct was prepared in pBluescript from three positive library clones. The *Eco*RI insert was ligated into pGH19 for expression in *Xenopus* oocytes. To prepare the human–snake chimaeric construct, regions within $hNa_V1.4$/pSP64T were replaced with Benton $tsNa_V1.4$ by using a modified three-fragment PCR overlap extension: in domain I, $tsNa_V1.4$ residues 275–414 for $hNa_V1.4$ residues 277–424; in domain II, $tsNa_V1.4$ residues 761–814 for $hNa_V1.4$ residues 724–777; in domain III, $tsNa_V1.4$ residues 1,111–1,298 for $hNa_V1.4$ residues 1,185–1,269; and in domain IV, $tsNa_V1.4$ residues 1,537–1,603 for $hNa_V1.4$ residues 1,508–1,574. Other constructs were prepared by a two-fragment PCR overlap extension method of site-directed mutagenesis with substitutions at the positions shown in Fig. 1b. A second Willow Creek construct was prepared with a V1561I substitution. Amplified regions were verified by automated DNA sequencing.

Oocyte expression and electrophysiology

Capped RNAs were synthesized and purified (mMessage mMachine kit; Ambion). *Xenopus laevis* oocytes were collected and injected with 27 ng of each cRNA.

Ionic currents were measured at room temperature (22–25 °C) 2–10 days after cRNA injection by using the cut-open oocyte Vaseline gap voltage-clamp technique[30] with a CA-1B High Performance Oocyte Clamp (Dagan Instruments). Recordings were made in an external solution containing (in mM): 120 Na-Mes, 10 Hepes-Na, 1.8 $CaCl_2$, pH 7.2, and an internal solution containing (in mM): 110 K-Mes, 10 Na-Mes, 10 Hepes-K, 1 EGTA, pH 7.2.

Current records were acquired using Pulse software (HEKA), sampling at 100 kHz and filtering at 20 kHz. Peak currents were evoked at 0.05 Hz with 20-ms pulses to 0 mV following a 200-ms prepulse to −120 mV. The holding potential for all experiments was −100 mV. Leak subtraction was performed before the test pulse (p) with the use of a $p/4$ protocol. Peak current amplitudes were measured offline with PulseFit (HEKA). The ratios of peak currents in the presence and absence of TTX over a range of TTX concentrations were calculated with peak currents recorded before and after perfusing the selected TTX concentration into the external bath solution for 5 min. To estimate the TTX concentration that blocked 50% of the expressed channels, the data were fitted to an equation derived from a single-site Langmuir adsorption isotherm: current ratio $= K_d/(K_d+[TTX])$, in which [TTX] is the concentration of toxin and K_d is the concentration of TTX at which half of the receptors are bound to the toxin. Statistical analyses were conducted with PROC NLIN in SAS/STAT version 9.0. K_d and its 95% confidence limits were estimated from the curve.

Received 14 January; accepted 10 February 2005; doi:10.1038/nature03444.

1. Rausher, M. D., Miller, R. E. & Tiffin, P. Patterns of evolutionary rate variation among genes of the anthocyanin biosynthetic pathway. *Mol. Biol. Evol.* **16,** 266–274 (1999).
2. Schluter, D., Clifford, E. A., Nemethy, M. & McKinnon, J. S. Parallel evolution and inheritance of quantitative traits. *Am. Nat.* **163,** 809–822 (2004).
3. Stern, D. L. Evolutionary developmental biology and the problem of variation. *Evolution* **54,** 1079–1091 (2000).
4. Brodie, E. D. Jr, Ridenhour, B. J. & Brodie, E. D. III The evolutionary response of predators to dangerous prey: hotspots and coldspots in the geographic mosaic of coevolution between garter snakes and newts. *Evolution* **56,** 2067–2082 (2002).
5. Beldade, P., Brakefield, P. M. & Long, A. D. Contribution of Distal-less to quantitative variation in butterfly eyespots. *Nature* **415,** 315–318 (2002).
6. Abzhanov, A., Protas, M., Grant, B. R., Grant, P. R. & Tabin, C. J. Bmp4 and morphological variation of beaks in Darwin's finches. *Science* **305,** 1462–1465 (2004).
7. Shapiro, M. D. *et al.* Genetic and developmental basis of evolutionary pelvic reduction in threespine sticklebacks. *Nature* **428,** 717–723 (2004).
8. Yamamoto, Y., Stock, D. W. & Jeffery, W. R. Hedgehog signalling controls eye degeneration in blind cavefish. *Nature* **431,** 844–847 (2004).
9. Hoekstra, H. E. & Nachman, M. W. Different genes underlie adaptive melanism in different populations of rock pocket mice. *Mol. Ecol.* **12,** 1185–1194 (2003).
10. ffrench-Constant, R. H., Daborn, P. J. & Le Goff, G. The genetics and genomics of insecticide resistance. *Trends Genet.* **20,** 163–170 (2004).
11. Hille, B. *Ion Channels of Excitable Membranes* (Sinauer, Sunderland, Massachusetts, 2001).
12. Brodie, E. D. III & Brodie, E. D. Jr Predator–prey arms races: asymmetrical selection on predators and prey may be reduced when prey are dangerous. *Bioscience* **49,** 557–568 (1999).
13. Janzen, F. J., Krenz, J. G., Haselkorn, T. S., Brodie, E. D. & Brodie, E. D. Molecular phylogeography of common garter snakes (*Thamnophis sirtalis*) in western North America: implications for regional historical forces. *Mol. Ecol.* **11,** 1739–1751 (2002).
14. Geffeney, S., Brodie, E. D. Jr, Ruben, P. C. & Brodie, E. D. III Mechanisms of adaptation in a predator-prey arms race: TTX-resistant sodium channels. *Science* **297,** 1336–1339 (2002).

15. Satin, J. *et al.* A mutant of TTX-resistant cardiac sodium channels with TTX-sensitive properties. *Science* **256,** 1202–1205 (1992).
16. Kaneko, Y., Matsumoto, G. & Hanyu, Y. TTX resistivity of Na^+ channel in newt retinal neuron. *Biochem. Biophys. Res. Commun.* **240,** 651–656 (1997).
17. Yotsu-Yamashita, M. *et al.* Binding properties of ^{3}H-PbTx-3 and ^{3}H-saxitoxin to brain membranes and to skeletal muscle membranes of puffer fish *Fugu pardalis* and the primary structure of a voltage-gated Na^+ channel alpha-subunit (fMNa1) from skeletal muscle of *F. pardalis*. *Biochem. Biophys. Res. Commun.* **267,** 403–412 (2000).
18. Terlau, H. *et al.* Mapping the site of block by tetrodotoxin and saxitoxin of sodium channel II. *FEBS Lett.* **293,** 93–96 (1991).
19. Yamagishi, T., Li, R. A., Hsu, K., Marban, E. & Tomaselli, G. F. Molecular architecture of the voltage-dependent Na channel: functional evidence for alpha helices in the pore. *J. Gen. Phys.* **118,** 171–181 (2001).
20. Kallen, R. G. *et al.* Primary structure and expression of a sodium channel characteristic of denervated and immature rat skeletal muscle. *Neuron* **4,** 233–242 (1990).
21. Trimmer, J. S., Cooperman, S. S., Agnew, W. S. & Mandel, G. Regulation of muscle sodium channel transcripts during development and in response to denervation. *Dev. Biol.* **142,** 360–367 (1990).
22. Huey, R. B. & Moody, W. J. Neuroscience and evolution. Snake sodium channels resist TTX arrest. *Science* **297,** 1289–1290 (2002).
23. Zakon, H. H. Convergent evolution on the molecular level. *Brain Behav. Evol.* **59,** 250–261 (2002).
24. Lipkind, G. M. & Fozzard, H. A. KcsA crystal structure as framework for a molecular model of the Na^+ channel pore. *Biochemistry* **39,** 8161–8170 (2000).
25. Plummer, N. W. & Meisler, M. H. Evolution and diversity of mammalian sodium channel genes. *Genomics* **57,** 323–331 (1999).
26. Raymond, C. K. *et al.* Expression of alternatively spliced sodium channel alpha-subnit genes: Unique splicing patterns are observed in dorsal root ganglia. *J. Biol. Chem.* **279,** 46234–46241 (2004).
27. Goldin, A. L. Resurgence of sodium channel research. *Annu. Rev. Physiol.* **63,** 871–894 (2001).
28. Choudhary, G., Yotsu-Yamashita, M., Shang, L., Yasumoto, T. & Dudley, S. C. Jr Interactions of the C-11 hydroxyl of tetrodotoxin with the sodium channel outer vestibule. *Biophys. J.* **84,** 287–294 (2003).
29. Penzotti, J. L., Fozzard, H. A., Lipkind, G. M. & Dudley, S. C. Jr Differences in saxitoxin and tetrodotoxin binding revealed by mutagenesis of the Na^+ channel outer vestibule. *Biophys. J.* **75,** 2647–2657 (1998).
30. Stefani, E. & Bezanilla, F. Cut-open oocyte voltage-clamp technique. *Methods Enzymol.* **293,** 300–318 (1998).

Supplementary Information accompanies the paper on **www.nature.com/nature**.

Acknowledgements We thank A. Correa for advice regarding the cut-open oocyte voltage clamp; S. Durham for advice regarding the statistical analysis; C. Feldman and M. Pfrender for advice regarding the phylogenetic analysis; J. Caldwell for primers; A. Goldin for sharing his sodium channel sequence alignment; and C. Hanifin and the USU herpetology group for comments that improved the manuscript. This work was supported by research grants from the National Institute of Health (P.C.R.) and from the National Science Foundation (E.D.B. Jr and E.D.B. III).

Competing interests statement The authors declare that they have no competing financial interests.

Correspondence and requests for materials should be addressed to S.L.G. (geffeney@biology.usu.edu). Sequences described in this paper have been deposited in GenBank under accession numbers AY851743, AY851744, AY851745 and AY851746.

Sodium channel mutation leading to saxitoxin resistance in clams increases risk of PSP

V. Monica Bricelj[1], Laurie Connell[2], Keiichi Konoki[3], Scott P. MacQuarrie[1], Todd Scheuer[3], William A. Catterall[3] & Vera L. Trainer[4]

[1]*Institute for Marine Biosciences, National Research Council, Halifax, Nova Scotia B3H 3Z1, Canada*
[2]*School of Marine Sciences, University of Maine, Orono, Maine 04469, USA*
[3]*Department of Pharmacology, University of Washington, Seattle, Washington 98195, USA*
[4]*NOAA Fisheries, Northwest Fisheries Science Center, Seattle, Washington 98112, USA*

Bivalve molluscs, the primary vectors of paralytic shellfish poisoning (PSP) in humans, show marked inter-species variation in their capacity to accumulate PSP toxins (PSTs)[1] which has a neural basis[2,3]. PSTs cause human fatalities by blocking sodium conductance in nerve fibres[4,5]. Here we identify a molecular basis for inter-population variation in PSP resistance within a species, consistent with genetic adaptation to PSTs. Softshell clams (*Mya arenaria*) from areas exposed to 'red tides' are more resistant to PSTs, as demonstrated by whole-nerve assays, and accumulate toxins at greater rates than sensitive clams from unexposed areas. PSTs lead to selective mortality of sensitive clams. Resistance is caused by natural mutation of a single amino acid residue, which causes a 1,000-fold decrease in affinity at the saxitoxin-binding site in the sodium channel pore of resistant, but not sensitive, clams. Thus PSTs might act as potent natural selection agents, leading to greater toxin resistance in clam populations and increased risk of PSP in humans. Furthermore, global expansion of PSP to previously unaffected coastal areas[6] might result in long-term changes to communities and ecosystems.

PSP, caused by human consumption of shellfish that feed on toxic algae, is a public health hazard and causes severe economic losses globally due to bans on harvesting of contaminated shellfish and the need for costly monitoring programmes. PSP-producing dinoflagellates (for example *Alexandrium* spp.) cause toxic blooms ('red tides') in North America and worldwide. PSTs block conduction of the nerve impulse by interfering with the voltage-dependent increase in sodium-ion conductance that generates the action potential in nerve and muscle fibres[4,5], leading to neuromuscular paralysis. Large differences in PST accumulation between bivalve species *in vivo*[1] have been associated with *in vitro* differences in sensitivity of isolated nerves to saxitoxin (STX), the most potent PST, and the related tetrodotoxin (TTX)[2,3]. STX and TTX bind to a single site in the outer pore of the Na^+ channel, formed by the amino-acid residues in the outer-pore loops located between the S5 and S6 segments of each of the four homologous domains (I–IV) of the α-subunit[7,8]. Could differences in amino acid sequence in the receptor site for STX and TTX in Na^+ channels cause differences

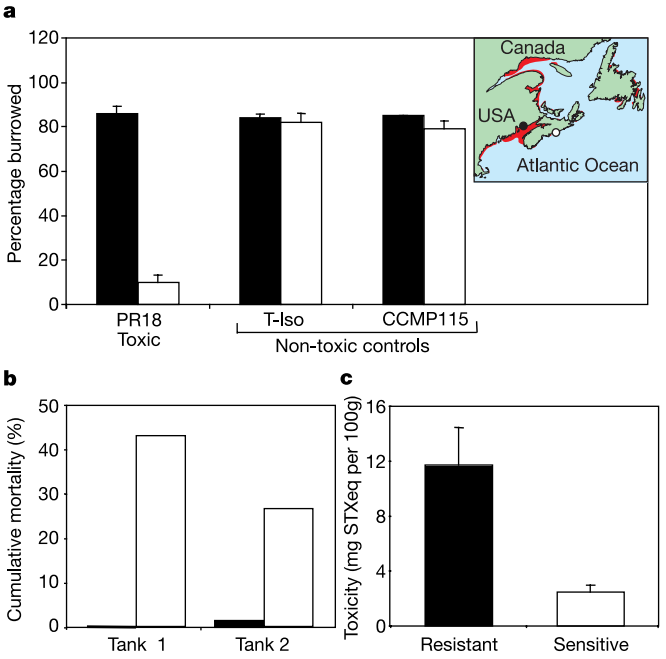

Figure 1 Responses to PSTs in two *M. arenaria* populations. **a**, Percentage of clams that burrowed after 24 h of exposure to *A. tamarense* (strains PR18b or CCMP115) or *I. galbana* (T-Iso) ($n = 2$ tanks). Map shows the study sites BF (filled circle) and LE (open circle); the PSP-affected coastline is in red. **b**, Mortality after 16 days of toxification with strain PR18b (determined by visual inspection (dead clams removed) (tank 1) and by removal of all clams every 2 days (live clams reintroduced in sediment) (tank 2)). In **a** and **b**, filled columns are results for BF clams, and open columns for LE clams. **c**, Tissue toxicity of live clams after 16 days of toxification of resistant BF and sensitive LE clams (burrowers and non-burrowers at 24-h, respectively). All results are means ± s.e.m.